A Novel Device Decoupling Tactile Slip and Hand Motion in Reaching Tasks: The HaptiTrack Device

Simone Ciotti†, Colleen P. Ryan†, Matteo Bianchi, Francesco Lacquaniti, and Alessandro Moscatelli

***Abstract*— Hand reaching is a complex task that requires the integration of multiple sensory information from muscle, joints and the skin, and an internal model of the motor command. Recent studies in neuroscience highlighted the important role of touch for the control of hand movement while reaching for a target. We present a novel device, the *HaptiTrack* device, to physically decouple tactile slip motion and hand movements. The new device generates precisely controlled 2D motion of a contact plate, measures contact forces, and provides hand and finger tracking through an external tracking system. By means of a control algorithm described in this manuscript, the velocity of tactile slip can be changed independently from the velocity of the hand sliding on the device's surface. Due to these multiple features, the device can be a powerful tool for the evaluation of tactile sense during hand reaching movements in healthy and pathological conditions.**

***Index Terms*— Haptic Display, Neuroscience, System Design and Analysis, Perception and Psychophysics, Tactile Devices, Tactile Display**

I. Introduction

Studies in neuroscience highlighted the crosstalk between the sense of touch and the motor control of the hand. During the exploratory procedures, the movements of the hands aim to maximize the information about the touched objects [1]. Moreover, cutaneous information provides an important feedback to control hand movements in reaching [2] and in manipulation tasks [3]. In our previous study, we changed surface texture to independently manipulate tactile and hand motion, and this produced a systematic error in the reaching direction [2]. The relationship between touch and movement control has an important implication in clinical settings. Accordingly, several neurological and metabolic diseases are characterized by complex dysfunctions in both the motor and the somatosensory system [4].

Hand reaching is a complex task that requires the integration of multiple sensory information from muscle, joints and the skin, and internal model of the motor command [5][6][7]. *Ad-hoc* devices are necessary to study the contribution of touch for the control of hand movements. Dostmohamed and Hayward developed a simple, yet highly-effective device that can render surfaces of different shapes by controlling the tilt angle of the contact plate in relation to the back-and-forth movement of the participant on a slide [8]. In [9], the authors developed a device to evaluate the contribution of the sense of touch in tool use, to provide information about changes in the location of the targets to be reached. The Latero device (Tactile Labs, Inc.) can render the sensation of a surface moving across the skin from the sequential vibrations of multiple pins. This has been used in the past for the evaluation of tactile motion during hand movements [10] [11]. Due to the small size of active surface of the device, only a limited portion of the skin at a time can be stimulated—typically, the fingertip pulp. Other devices are able to deliver slip motion stimuli along a single or multiple directions, with high degree of precision [12] [13]. These devices have been used mostly for the evaluation of passive touch, where the participants contact the movable surface with the static hand kept in place by a finger holder.

We present a novel device, the *HaptiTrack* device, that can physically decouple tactile and hand motion during reaching movement. That is, the velocity of tactile slip can be changed independently from the velocity of the hand sliding on the device's surface. The apparatus provides hand and finger tracking during reaching tasks, while generating precisely controlled 2D motion of a large contact plate. By changing a single gain parameter of the control algorithm, the device is able to fully decouple the slip motion from the hand velocity during reaching movements.

In this manuscript we characterized the response of the device during a visually-guided reaching task. The position and the velocity of the participants' finger, the contact force on the movable plate, and the trajectory of the plate were measured by means of the different sensors of the apparatus. We aimed to change the tactile feedback during the reaching task, with low mechanical interference with the limb motion. To this end, we reduced the friction coefficient by covering the contact plate with Teflon (hydrophobic polytetrafluoroethylene; PTFE) and by lubricating it. We analyzed the relationship between tangential forces and load force and motion speed because these are known to affect the frictional properties of the skin [14]. A preliminary version of the device was presented at the conference ICNR2020, in which only one axis was actuated and vibration transmission analysis was performed [15].

II. Methods

A. Hardware & Software Description

The HaptiTrack device is illustrated in Fig. 1(a) and consists of a motion capture system, a sensorized plate, and

† These authors contributed equally to the work

Authors S. C., C.P.R., F.L., A.M. are with Department of Systems Medicine and Center of Space Biomedicine, University of Rome Tor Vergata, Rome, Italy and with Laboratory of Neuromotor Physiology, IRCCS Fondazione Santa Lucia, Rome, Italy (corresponding author to provide e-mail: ciottisimone88@gmail.com).

Authors M. B. is with the Reasearch Center "E. Piaggio" University of Pisa, Pisa 56126, Italy, and also with the Department of Information Engineering of University of Pisa, 56122 Pisa, Italy.

This article has been accepted for publication in a future issue of this journal, but has not been fully edited. Content may change prior to final publication. Citation information: DOI 10.1109/TOH.2021.3075024, IEEE Transactions on Haptics

two perpendicular linear motion axes actuated by DC-motors controlling the position of the plate.

The OptiTrack motion capture system consists of four Flex13 cameras and an OptiHub synchronization box firmly attached to the metal frame. The motion capture system has a frame rate of 120 FPS, and a declared mean position reconstruction error less than 1 mm. The OptiTrack system is used to track two ABS-printed rigid bodies: (i) a thimble by means of 5 OptiTrack markers (diameter: 3 mm) and (ii) the circular plate of the sensorized surface (radius: 100 mm, thick: 2 mm), by means of four OptiTrack markers placed along its circumference. Fig. 1(b) shows the thimble attached to the participant's finger.

The sensorized plate is mounted on the top of the apparatus, as shown in Fig. 1(b). This is composed of: (i) a base to connect the top single-axis to the sensorized plate; (ii) a 6-axis force/torque sensor ATI Mini45 in the middle; (iii) the circular plate printed in ABS and covered with a PTFE layer. PTFE has a very low friction coefficient, between $0.05 - 0.1$ [16]. To attenuate vibrations, four MISUMI damping components (GELB1401) are mounted between the top single-axis and the sensorized surface. The ATI Mini45 6-axis force/torque sensor has a compact, low-profile design with a high signal-to-noise ratio. This sensor has been used to investigate human touch in exploratory and reaching tasks in previous studies [17]. The control box of the ATI was attached to the metal frame of the apparatus.

The movement of the sensorized plate is produced by two perpendicular linear motion axes mounted on top of each other, similar to a 2D pantograph. Each axis consists of a MISUMI compact single-axis actuator (LX3005CP-MX-B1-N-600-FA2) driven by a Maxon motor (DCX26L GB KL 24V with planetary gearhead GPX26 C 3.9:1) coupled to the single-axis through a Nabeya Bi-tech vibrations absorption coupling (XGS-25CS-6-6). For each motor, the angular position is controlled by means of a qbrobotics SoftHand v1.0 control board, endowed with the manufacture firmware, with the actual position measured by a 16-bit resolution position encoder placed at the end of the ball screw. Besides others functionalities, the SoftHand board provides the implementation of a Proportional–Integral–Derivative (PID) control with custom parameters and a fixed refresh rate of 1 kHz.

The *HaptiTrack* allows a maximum speed of 150 mm/s with motor generated vibrations frequency equal to 30 Hz. The maximum speed and vibrations produced by the motors are function of the motor no-load speed of 1795 RPM and of the single-axis actuator ball screw lead of 5 mm. For sake of safety, each axis is endowed at each stroke extremity with a Panasonic rectangular-shaped inductive proximity sensor (GX-F12A), for a total of 4 sensors 5 V powered through a USB cable. Proximity sensors signals are summed together, hence, the resulting signal is used as control input of a SparkFun relay (Beefcake Relay Control Kit Ver. 2.0) to immediately interrupt the motors power supply if any of proximity sensors is covered by any of the moving parts.

A wood panel with a hole in the center (not shown in the figure) is mounted in the front side of the frame. A black curtain in front of the hole occluded the hand and the surface motion from sight. Visual feedback was displayed to the participant on a PC monitor attached to the back side of the frame. The use of an external monitor is due to the restrictions related to the Covid-19 pandemic; in the future this can be replaced by a Head Mounted Display.

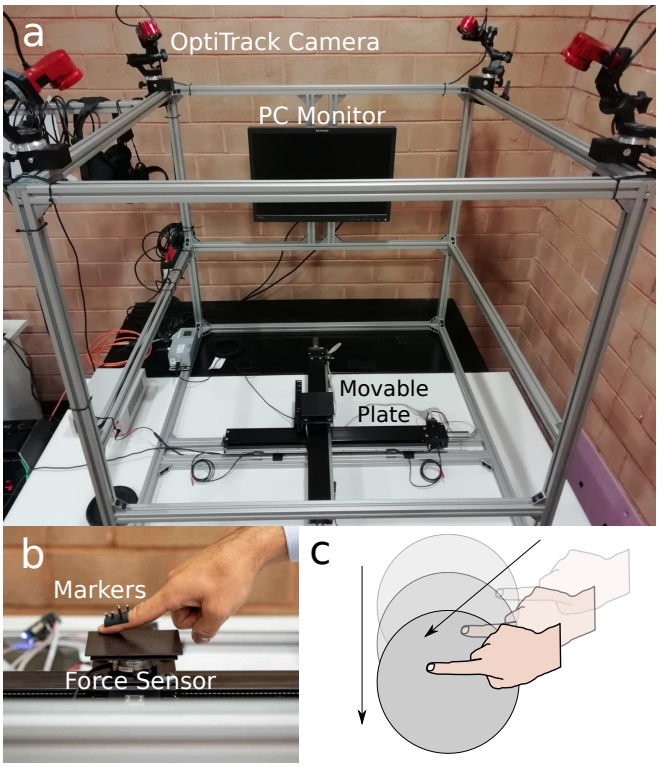

Fig. 1. (a) The HaptiTrack device inside the metal frame with mounted an OptiTrack Flex13 camera in each corner. (b) The sensorized plate composed of the 6-axis force/torque sensor and the movable plate. (c) A graphical example of the performed task. The circular plate was removed from the picture for a better visualization of the other components.

For each main hardware component a C++ library was developed under the 3-clause BSD license, a permissive free software license. A core C++ software with a sampling rate of 200 Hz integrates all libraries and controls the virtual environment developed with Unreal Engine 4. The sampling rate was chosen to obtain a satisfactory force/torque sampling and sensorized plate position updates. A higher sampling rate was not possible due to the limit imposed by the OptiTrack system, whose refresh rate is equal to 120 Hz. Instead, the refresh rate of the qbrobotics control boards controlling the angular position of the motors is imposed by the manufacture firmware and it is equal to 1 kHz.

B. System Performance Identification

A position PID controller was set for each axis of motion. PID parameters were chosen in a trial-and-error procedure aiming to: (i) reduce the vibrations transmitted to the sensorized plate, as reported in [15], (ii) generate a smooth trajectory-following of an OptiTrack rigid-body, and (iii) minimize the position error within the constrains of the mechanical components.

This article has been accepted for publication in a future issue of this journal, but has not been fully edited. Content may change prior to final publication. Citation information: DOI 10.1109/TOH.2021.3075024, IEEE Transactions on Haptics

The closed-loop frequency response of the apparatus was investigated applying as position input an exponential chirp signal one time with the maximum amplitude of 100 mm, and the second one with an amplitude of 50 mm, which is consistent with the displacement required in the user study, as reported in Section II-C. An open-loop system characterization was not performed to avoid an unstable HaptiTrack moving behavior.

For both amplitudes, the chirp signal has a total duration of 300 s, and a minimum and maximum motion speed of 10 mm/s and 400 mm/s, respectively. The chirp frequency rate update is 0.025 Hz and 0.05 Hz, for the maximum amplitude and the half-maximum one, respectively. Movement amplitude (A), motion speed (v), and frequency (f) are related by the equation $f = v/(4 * A)$.

In the performed test, at each software control step, a new position reference from the generated chirp signal is provided to the qbrobotics control board, hence, the sensorized plate position is measured by the OptiTrack rigid-body composed of the four markers placed along the plate circumference. For each movement amplitude and tested frequency (motion speed), the HaptiTrack performance was computed from the ratio between the plate position measured from the OptiTrack and the target position.

C. User study: visually guided reaching task

In a pilot experiment, we evaluated the capacity of the device to decouple hand movements and tactile slip motion in a visually-guided reaching task. The first aim of this experiment was to characterize the response of the device during self-paced hand movements. A second aim was to evaluate the contact force and velocity of the hand movement in the different experimental conditions. Five right-handed participants performed the task (age: 32 ± 5; mean $\pm$ sd; 1 female and 4 males). The pilot experiment consisted of 135 trials. In each trial, the participant slid their index fingertip on the sensorized plate, from a starting position towards a virtual target. A visual plate having the same size as the sensorized plate of the apparatus was always visible on the PC monitor in front of the participant. In each trial, one of three virtual targets was pseudo-randomly chosen and presented to the participants. The three virtual targets were placed on a circumference (not displayed on the screen) with radius of 60 mm at $\pm 45°$ and $0°$ w.r.t. the participant, with $0°$ being in front of the participant. To avoid reaching the border of the sensorized plate, the visual plate changed color when motion path exceeded the threshold value of 80 mm.

Before trial onset, the sensorized plate was moved to the center of the testing apparatus corresponding to the OptiTrack zero-position on the 2D plane. Then, the participant touched the teflon sheet on the plate and a grey sphere (diameter 10 mm) appeared on the screen. The relative position of the grey sphere on the visual plate corresponded to the position of the participant's fingertip on the Teflon plate. The position of the grey sphere was update every 5 ms to provide a visual feedback on the finger displacement on the plate. A cyan disc with a radius of 1 mm identified

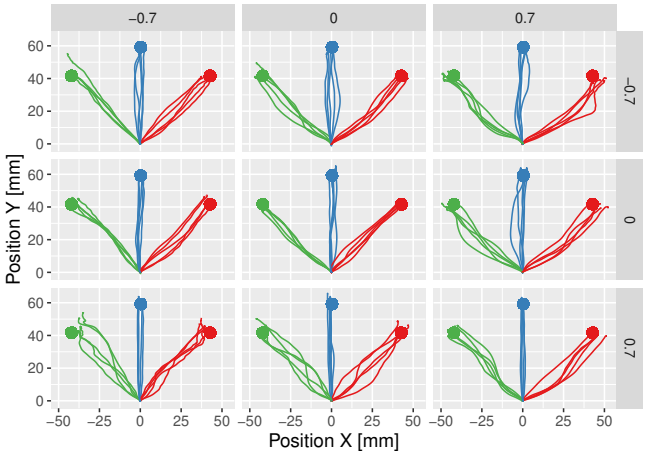

Fig. 2. Trajectories for different targets in a representative participant. Left, central, and right target are represented in different colors. In each panel, the labels on the x and the y axis indicate the corresponding value of x and y gain.

the starting position. When the participants reached the starting position, the cyan disc disappeared and a green sphere (diameter: 10 mm) identifying the target to reach was shown. Participants were instructed to reach the target—i.e., to match the position of the green sphere (the target) and the grey sphere (the fingertip) on the screen. The trial was over when participants lifted their finger from the sensorized plate. During the trial, if the normal force was above the threshold value of 0.3 N (contact-on), the 2D position of the plate was updated every 5 ms according to the Eq. 1.

$$\begin{bmatrix} x \\ y \end{bmatrix}_{new} = \begin{bmatrix} x \\ y \end{bmatrix}_{old} + \begin{bmatrix} \gamma_x & 0 \\ 0 & \gamma_y \end{bmatrix} \left(\begin{bmatrix} X \\ Y \end{bmatrix}_{new} - \begin{bmatrix} X \\ Y \end{bmatrix}_{old} \right), \quad (1)$$

where subscript *new* identifies the current position, and subscript *old* the previous one; lowercase x, and y stand for the x and y plate position, respectively; uppercase letters specify finger position measured with the OptiTrack; γ_x and γ_y identifies gains between the participant's finger and the contact surface. The gains change pseudo-randomly across trials among three values: $-0.7, 0, 0.7$. As illustrated in Fig. 4, the plate moved along different directions in response to hand motion, depending on the values of γ_x and γ_y. In each trial, after the participant reached the starting position, all position variables were initialized at the current finger or plate position, respectively.

At the beginning of the experimental session, the plate was lubricated to reduce the shear force on the fingertip. At the end of the trial, if the applied normal force was above 2 N the screen became red for 2 s to prompt the participant to reduce the contact force in the next trial.

D. Data Analysis

The analysis was performed in R version 4.0.4 [18]. Position, velocity, and force signals where filtered with Butterwoth 5^{th} order filter (cut-off frequency of 10 Hz). For each participant we computed the Pearson correlation

This article has been accepted for publication in a future issue of this journal, but has not been fully edited. Content may change prior to final publication. Citation information: DOI 10.1109/TOH.2021.3075024, IEEE Transactions on Haptics

between the required and the actual position of the plate. In each trial, we collected the peak value of the tangential force components for further analysis. Tactile velocity was computed as the signed difference between the velocity of the plate and the velocity of the hand. Separately for the x and the y axis, we fit a Linear Mixed Model to study the relationship between tangential force peak $|F_t|$ and tactile speed S_t (i.e., the module of the tactile velocity) and load force F_z (see Eq. 2).

$$|F_t| = \beta_0 + \beta_1 S_t + \beta_2 F_z + u_i, \tag{2}$$

where β_0, β_1, and β_2 are the fixed-effect coefficient of the model, and u_i is the random-effect predictor accounting for the variability between participants. We used the absolute value of force to analyze together the trials towards left and right targets.

III. Results

A. System Performance Identification

Fig. 3 shows, for the two test amplitudes, the frequency response magnitude for the x and the y axis. For the two axes, the attenuation is close to zero within the peak speed tested in the user study (150 mm/s, corresponding to a frequency of about 0.37 Hz and 0.75 Hz for the large and the small test amplitude, respectively). The y-axis shows a near-to-zero, quasi-constant attenuation for lower frequencies, till the cut-off frequency from which the response is attenuated proportionally to the stimulation frequency, due to motor speed limit. The x-axis presents a small attenuation at very low frequencies, an oscillation around the 0 dB for mid-work frequencies, and a higher attenuation at higher frequencies. The slightly worse performance of the x-axis at low frequency could be improved by adjusting the relative PID controller, to compensate for the higher inertia of the axis.

B. User study: visually guided reaching task

The motion paths in a representative participant are illustrated in Fig. 2. To characterize the apparatus, we analyzed the relationship between the finger position (shown in red in Fig. 4), the required, and the actual plate position (shown in blue and in green in the figure, respectively). The Fig. 4 illustrates the motion path for individual trials, for target at $-45°$, and different values of x and y gain. The actual position of the plate (measured from the motor encoders) is consistent with the one required by Eq. 1.

Next, we computed the correlation between the required and the actual position of the plate for all participants together. The correlation median values are 0.998 and 0.999 for x and y axis, respectively, and they are equal to one for most of the trials.

Fig. 5 illustrates the position lag, computed for every sampling step (i.e, every 5 ms), as the norm of the difference between the required and actual surface position (one participant). The position lags were similar for all target orientations. There is a larger position lag during the initial

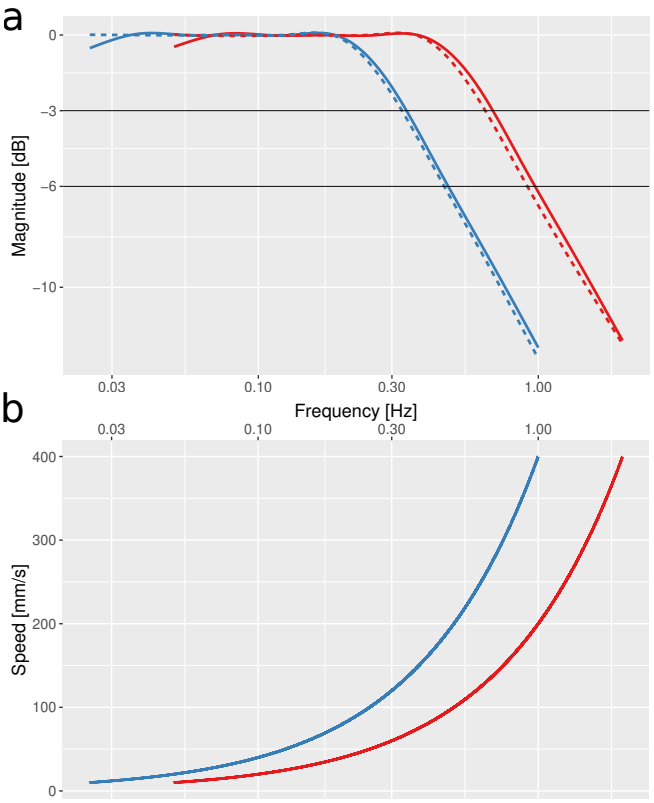

Fig. 3. (a) Frequency response magnitude for each axis (i.e., x-axis solid line, y-axis dashed line) at each test amplitude (i.e., blue 100 mm, red 50 mm). (b) Move speed - frequency relation with respect to the movement amplitude (i.e., blue 100 mm, red 50 mm). For both plots the frequency is plotted in logarithmic scale.

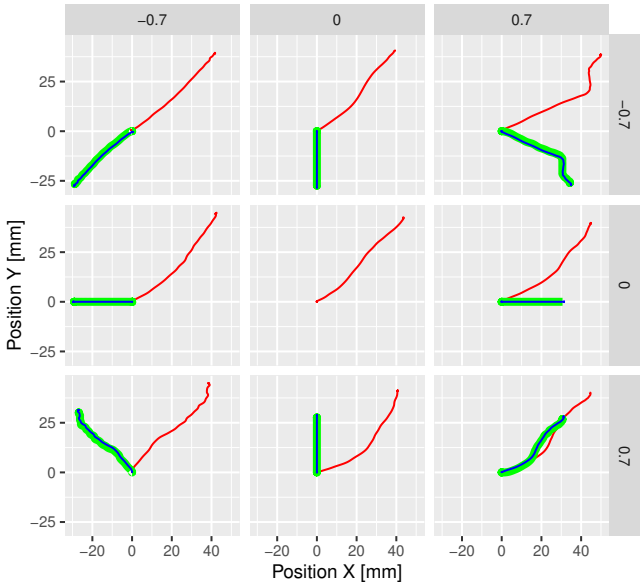

Fig. 4. Trajectories for different gain combination for target at $-45°$. In red the finger trajectory, in green the actual plate trajectory, and in blue the required plate trajectory. In each panel, the labels on the x and the y axis indicate the corresponding value of x and y gain.

This article has been accepted for publication in a future issue of this journal, but has not been fully edited. Content may change prior to final publication. Citation information: DOI 10.1109/TOH.2021.3075024, IEEE Transactions on Haptics

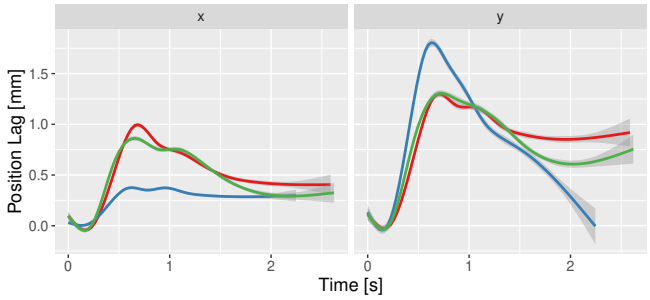

Fig. 5. Contact surface position lag for x and y axis with the color code identifying the target (i.e., $-45°$ in red, $0°$ in blue, and $+45°$ in green), for a participant (data interpolated across trials with GAM method, shaded area represents the 95% confidence intervals). The position lag is computed as the norm of the difference between the required and the actual position.

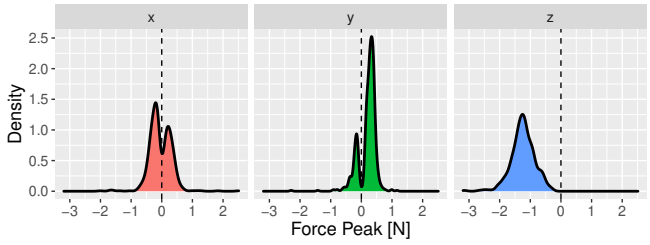

Fig. 6. Force distribution along each axis and for all participants together.

transient phase until approximately $0.5\ s$. This is possibly due to the inertia of the ball screw, and to the time constant of the motors. After the transient phase, the position lag trends to drop, but never reaches a zero value. This behavior can be associated to a fixed error due to the implemented position control PID, to the mechanical components, and to the latency time of the tracking system.

In the design of the experiment, we took precautions to ensure a low value of shear force during the reaching movement, that is, we used a Teflon sheet covered with lubricant. We analyzed the contact force to verify that shear force was low in all experimental conditions. In each trial we filtered the data, as explained in Section II-D, and saved the signed value of the force peak separately for each axis. The distribution of the force peak is always less than $1\ N$ on x and y axis, and less than the threshold of $2\ N$ along z-axis, as shown in Fig. 6. Along the x-axis there is a bimodal distribution which corresponds to the left (negative values) and right (positive values) direction of movement. Along the y-axis, there is a higher positive peak corresponding to a forward direction of movement. Some negative values are possibly due to backward correction movement. Along the z-axis the values are always unimodal and negative corresponding to the downward pressing of the finger.

We fit a linear model to study the relationship between tangential force peak and tactile slip speed and load force (see Eq. 2). The fit of the model is shown in Fig. 7 and Fig. 8. There is a significant association between the tactile slip speed and the tangential force peak, such that the faster the slip motion, the higher the tangential force (x-axis: $t = 16.6$, $p < 0.001$; y-axis: $t = 6.7$, $p < 0.001$). The tangential force is also significantly associated with the load force (x-axis: $t = -12.6$, $p < 0.001$; y-axis: $t = -14.3$, $p < 0.001$). Albeit significant, the effect size is small: in all but one participants, the range of tangential force is within the range 0–$0.5\ N$.

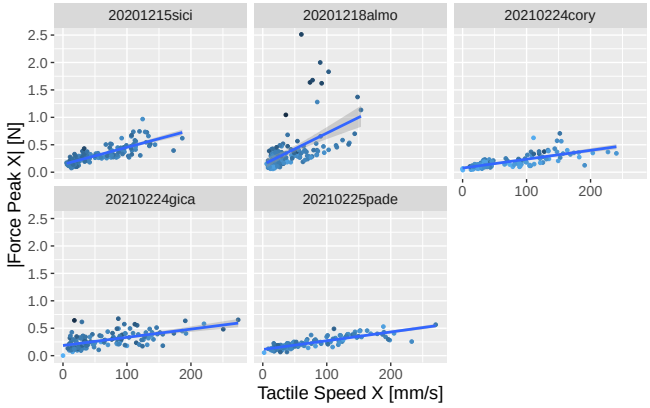

Fig. 7. Multiple linear regression model of force and speed (x-axis). The intensity of blue of each dot correspond to the value of load force (darker corresponding to higher load force). Participants are represented in different panels.

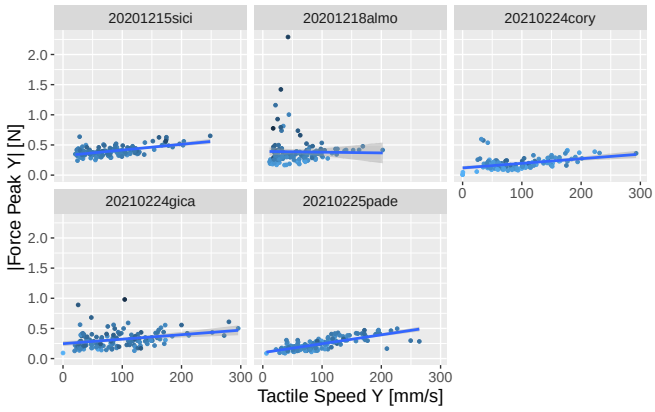

Fig. 8. Multiple linear regression model of force and speed (y-axis). The intensity of blue of each dot correspond to the value of load force (darker corresponding to higher load force). Participants are represented in different panels.

Finally, we analyzed the profiles of the finger velocity, shown in Fig. 9 for a participant. These are stereotyped and present a typical bell shape, in accordance with classical studies on motor control [7] [19]. The peak of the finger speed (i.e., the module of the finger velocity) was always less than $150\ mm/s$, the maximum admissible speed for the HaptiTrack device because of the hardware components.

IV. Discussion

We present a novel haptic device, the *HaptiTrack* device, that is able to physically decouple tactile motion from hand movement. In our previous studies, we *perceptually* decoupled tactile and proprioceptive signals by means of a motion illusion [2]. Instead, by using the HaptiTrack device, the two cues can be *physically* separated, by changing the

This article has been accepted for publication in a future issue of this journal, but has not been fully edited. Content may change prior to final publication. Citation information: DOI 10.1109/TOH.2021.3075024, IEEE Transactions on Haptics

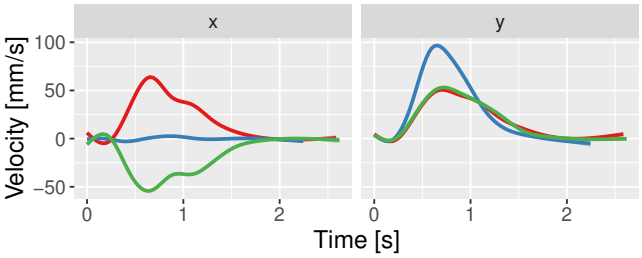

Fig. 9. The velocity of finger movement in a representative participant (data interpolated across trials with GAM method). Different colors identifies the three targets (i.e., $-45°$ in red, $0°$ in blue, and $+45°$ in green). In the frame of reference of the apparatus, a leftward movement (i.e. towards targets at $45°$) is coded as negative velocity and a rightward movement (targets at $-45°$) as positive.

gain parameter. Here we evaluated the trajectories of tactile motion during active reaching tasks for different values of the control gain. The device was able to produce the requested displacement of the plate, allowing us to fully decouple tactile slip from hand motion.

In the System Performance Identification analysis, the x-axis presents a slightly worse frequency response. This can be attributed to the greater inertia on the x-axis compared to the y-axis and to the choice of the position PID controller. In the future, an *ad-hoc* procedure will be developed to change the PID parameters for x-axis to compensate for its higher inertia. To increase the device performance, it will be possible to include the force and torque measurements in the control loop and update the plate position before a displacement of the finger has occurred, or adopting a different position control technique as a Model Predictive Control. Because of the low friction coefficient of the plate, lateral forces were very small, less than $0.5\ N$. In accordance with previous studies [14], we found a positive relationship between lateral force, load force, and motion speed. The viscosity of the lubricant and viscoelastic properties of the silicon dumpers may also explain the increase of lateral force with motion speed in our setup.

V. Future Work

In future work, the HaptiTrack device can provide an integrative method for testing sensorimotor functions in healthy individuals and in people affected by neurological diseases. To this end, it will be possible to reproduce the same reaching task presented here in the absence of visual feedback (the experiments are currently ongoing). We may use this apparatus to evaluate the integration of touch and proprioception in neurological diseases causing dysfunction of the somatosensory system, such as peripheral neuropathy, traumatic nerve injuries, multiple sclerosis, and stroke, to mention some [4]. This could pave the path to a novel clinical test where the precision of the reaching movement could be used to evaluate possible sensorimotor deficits in the participant.

Acknowledgments

This work was supported by the Italian Ministry of Health (Ricerca corrente, IRCCS Fondazione Santa Lucia), Italian Space Agency (grants I/006/06/0 and "MARS-PRE" 2019-11-U.0), and Italian University Ministry (PRIN grant "TIGHT", grant number 2017SB48FP and PRIN grant "NeuAge", grant number 2017CBF8NJ005).

References

[1] S. J. Lederman and R. L. Klatzky, "Hand movements: A window into haptic object recognition," *Cognitive psychology*, vol. 19, no. 3, pp. 342–368, 1987.

[2] A. Moscatelli, M. Bianchi, S. Ciotti, G. C. Bettelani, C. V. Parise, F. Lacquaniti, and A. Bicchi, "Touch as an auxiliary proprioceptive cue for movement control," *Science Advances*, vol. 5, no. 6, p. eaaw3121, jun 2019.

[3] R. S. Johansson and J. R. Flanagan, "Coding and use of tactile signals from the fingertips in object manipulation tasks," *Nature Reviews Neuroscience*, vol. 10, no. 5, pp. 345–359, 2009.

[4] A. H. Ropper, M. A. Samuels, and J. Klein, *Adams and Victor's principles of neurology*, eleventh edition ed. New York: McGraw-Hill Education, 2019.

[5] F. Lacquaniti and J. F. Soechting, "Coordination of arm and wrist motion during a reaching task," *Journal of Neuroscience*, vol. 2, no. 4, pp. 399–408, 1982.

[6] J. Gordon, M. F. Ghilardi, S. E. Cooper, and C. Ghez, "Accuracy of planar reaching movements," *Experimental brain research*, vol. 99, no. 1, pp. 112–130, 1994.

[7] P. Morasso, "Spatial control of arm movements," *Experimental brain research*, vol. 42, no. 2, pp. 223–227, 1981.

[8] H. Dostmohamed and V. Hayward, "Trajectory of contact region on the fingerpad gives the illusion of haptic shape," *Experimental Brain Research*, vol. 164, no. 3, pp. 387–394, 2005.

[9] J. A. Pruszynski, R. S. Johansson, and J. R. Flanagan, "A rapid tactile-motor reflex automatically guides reaching toward handheld objects," *Current Biology*, vol. 26, no. 6, pp. 788–792, 2016.

[10] L. Dupin, V. Hayward, and M. Wexler, "Direct coupling of haptic signals between hands," *Proceedings of the National Academy of Sciences*, vol. 112, no. 2, pp. 619–624, 2015.

[11] A. Moscatelli, V. Hayward, M. Wexler, and M. O. Ernst, "Illusory tactile motion perception: An analog of the visual filehne illusion," *Scientific reports*, vol. 5, no. 1, pp. 1–12, 2015.

[12] D. Gueorguiev, E. Vezzoli, A. Mouraux, B. Lemaire-Semail, and J.-L. Thonnard, "The tactile perception of transient changes in friction," *Journal of The Royal Society Interface*, vol. 14, no. 137, p. 20170641, 2017.

[13] A. Moscatelli, A. Naceri, and M. O. Ernst, "Path integration in tactile perception of shapes," *Behavioural Brain Research*, vol. 274, pp. 355–364, 2014.

[14] S. Derler and L.-C. Gerhardt, "Tribology of skin: review and analysis of experimental results for the friction coefficient of human skin," *Tribology Letters*, vol. 45, no. 1, pp. 1–27, 2012.

[15] S. Ciotti, M. Bianchi, D. Doria, F. Lacquaniti, and A. Moscatelli, "Haptitrack: A novel device for the evaluation of tactile sensitivity in active and in passive tasks," in *Proceedings of the 5th International Conference on NeuroRehabilitation*. Springer, in press, pp. 1–2.

[16] D. Flom and N. Porile, "Effects of temperature and high-speed sliding on the friction of 'teflon'on 'teflon'," *Nature*, vol. 175, no. 4459, pp. 682–682, 1955.

[17] B. Delhaye, V. Hayward, P. Lefevre, and J.-L. Thonnard, "Texture-induced vibrations in the forearm during tactile exploration." *Frontiers in behavioral neuroscience*, vol. 6, no. July, p. 37, jan 2012.

[18] R Core Team, *R: A Language and Environment for Statistical Computing*, R Foundation for Statistical Computing, Vienna, Austria, 2021. [Online]. Available: https://www.R-project.org/

[19] A. Goettker, K. Fiehler, and D. Voudouris, "Somatosensory target information is used for reaching but not for saccadic eye movements," *Journal of Neurophysiology*, vol. 124, no. 4, pp. 1092–1102, 2020.